Pressure-induced structural, electronic, and magnetic phase transitions in $FeCl_2$ studied by x-ray diffraction and resistivity measurements

G. Kh. Rozenberg,[1] M. P. Pasternak,[1] P. Gorodetsky,[1] W. M. Xu,[1] L. S. Dubrovinsky,[2] T. Le Bihan,[3] and R. D. Taylor[4]
[1]*School of Physics and Astronomy, Tel-Aviv University, Ramat-Aviv, 69978 Tel Aviv, Israel*
[2]*Bayerisches Geoinstitut, University Bayreuth, D-95440 Bayreuth, Germany*
[3]*European Synchrotron Radiation Facilities, BP 220, 38043 Grenoble Cedex, France*
[4]*MPA-10, MS-K764, Los Alamos National Laboratory, Los Alamos, New Mexico 87545, USA*
(Received 21 January 2009; published 9 June 2009)

High-pressure (HP) synchrotron x-ray diffraction (XRD) studies were carried out in $FeCl_2$ ($T_N \approx 24$ K) together with resistivity (R) studies at various temperatures and pressures to 65 GPa using diamond-anvil cells. This work follows a previous HP ^{57}Fe Mössbauer study in which two pressure-induced (PI) electronic transitions were found interpreted as: (i) quenching of the orbital-term contribution to the hyperfine field concurring with a tilting of the magnetic moment by 55°, and (ii) collapse of the magnetism concurring with a sharp decrease in the isomer shift. The $R(P,T)$ studies affirm that the cause of the collapse of the magnetism is a PI *p-d* correlation breakdown, leading to an insulator-metal transition at ~45 GPa and is not due to a spin crossover ($S=2 \rightarrow S=0$). The structure response to the pressure evolution of the two electronic phase transitions starting at *low pressures* (LP), through an *intermediate phase* (IP) 30–57 GPa, and culminating in a *high-pressure* phase, $P>32$ GPa, can clearly be quantified. The IP-HP phases coexist through the 32–57 GPa range in which the HP abundance increases monotonically at the expense of the IP phase. At the LP-IP interface no volume change is detected, yet the *c* axis increases and the *a* axis shrinks by 0.21 and 0.13 Å, respectively. The fit of the equation of state of the combined LP-IP phases yields a bulk modulus $K_0=35.3(1.8)$ GPa. The intralayer Cl-Cl distances increase but no change is observed in Fe-Cl bond length nor are there substantial changes in the interlayer spacing. The pressure-induced electronic IP-HP transition leads to a first-order structural phase transition characterized by a decrease in Fe-Cl bond length and an abrupt drop in $V(P)$ by ~3.5% accompanying the correlation breakdown. In this transition no symmetry change is detected and the XRD data could be satisfactorily fitted with the CdI_2 structure. The bulk modulus of the HP phase is practically the same as that of the LP-IP phases suggesting negligible changes in the phonon density of state.

DOI: 10.1103/PhysRevB.79.214105 PACS number(s): 61.50.Ks, 62.50.−p, 61.05.C−, 71.30.+h

I. INTRODUCTION

In the last decade there have been a number of high-pressure (HP) studies of properties of antiferromagnetic *Mott* insulators (MI),[1] the strongly *d-d* electronic-correlated transition-metal (TM) compounds. Most of the studies were performed in Fe compounds applying a variety of spectroscopic methods, x-ray diffraction (XRD), and transport measurements $R(P,T)$. The definitive electronic transition in MIs is the pressure-induced (PI) breakdown of the *Mott-Hubbard d-d* or *charge-transfer* (CT) *d-p* correlation energy leading to an insulator-metal transition concurrent with a collapse of magnetism. However, quite often within the correlated regime a spin crossover takes place, a high-spin to low-spin transition (HS-LS), resulting from a pressure-induced significant increase in the crystal field. For ferric systems this will result in a substantial decrease in magnetism due to $S=5/2 \rightarrow S=1/2$, and in ferrous systems a complete collapse of paramagnetism due to $S=2 \rightarrow S=0$ transition. The latter case has been observed in several ferrous oxides such as Wüstite (FeO),[2,3] $Mg_{1-x}Fe_xO$ (Ref. 4), and FeS.[5] However, this was not the case with ferrous iodide FeI_2,[6] where a correlation breakdown transition occurred at a relatively low pressure of ~20 GPa, as evidenced by ^{57}Fe-Mössbauer spectroscopy (MS) and $R(P,T)$ studies; XRD studies revealed an *isostructural* phase transition with ~5% volume reduction. The onset of correlation breakdown favoring an anticipated HS-LS transition may be related to the high degree of covalency, typical of a Fe-I bond, resulting in a relatively small CT energy gap. A correlation breakdown near 20 GPa has also been observed in isostructural NiI_2.[7]

An important feature of the CT transition in FeI_2 has been the formation of a structural precursor, an intermediate-pressure phase (IP) at 17 GPa with practically the same crystal volume but larger *c* and reduced *a* values.[8] According to ^{57}Fe MS data[6] a quenching of the orbital term takes place in the same pressure range. Since a contribution to the form and energy of the atomic interactions resulting from *spin-orbit* terms could be significant,[9] one might imply that the observed lattice distortion in the *c* direction is attributable to the same mechanism responsible for the orbital quenching. Studies of additional related systems may provide experimental support for this implication, namely, whether it is a general attribute of Fe-halide-layered structures or whether it takes place only in FeI_2.

A good candidate for such a study could be the antiferromagnetic insulator $FeCl_2$. At $P>0.6$ GPa $FeCl_2$ becomes isostructural to hexagonal FeI_2, the *h*-$FeCl_2$ phase [space-group $P\bar{3}m1$ (Ref. 10)] consisting of a sequence of -Cl-Fe-Cl−Cl-Fe-Cl- layers where the Cl-Cl layers are bound by weak Van der Waals forces (see Fig. 1). At temperatures below the Nèel temperature (T_N), Fe^{2+} moments at each sublattice align parallel and antiparallel, respectively, to the *c* axis.[11] As will be seen, this particular moment alignment

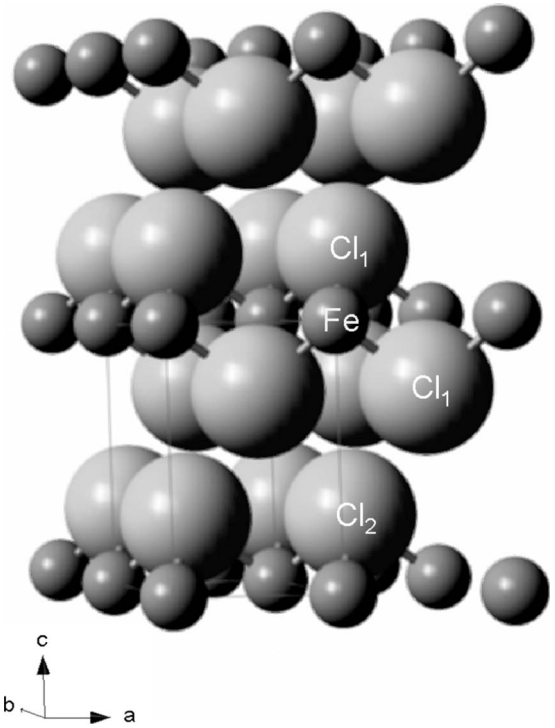

FIG. 1. The CdI_2-type crystal structure of $FeCl_2$ above ~0.6 GPa. The large and small spheres correspond to the Cl^{1-} and Fe^{2+} ions, respectively. The crystal is formed of *intralayer* covalently bonded Cl-Fe-Cl held together by Cl-Cl *interlayer* Van der Waal's forces.

probably originates from a significant contribution of the orbital term to the total ionic moment.

The layered $FeCl_2$ ionic compound is an ideal case study of: (i) structural response of a strongly correlated system to PI electronic changes, (ii) quenching of the orbital term, (iii) HS-LS transformation due to crystal-field (10 Dq) changes from the pressure increases, and ultimately, (iv) the *p-d* correlation breakdown. Recent HP Mössbauer studies[12] in $FeCl_2$ showed sound evidence, based on pressure dependencies of the magnetic hyperfine field (H_{hf}) and the isomer shift (IS), of the onset of a diamagnetic phase, signifying a total collapse of magnetism at $P>60$ GPa. This collapse of magnetism can be accounted for as either due to a spin crossover of Fe^{2+}, as in the case of FeO,[2,3] or to a correlation breakdown, as in the case of FeI_2.[6] These findings have led us to an elaborate HP study of the structural properties and interatomic distances based on careful XRD data analysis. To observe the occurrence of a PI insulator-metal transition, a critical feature of the correlation breakdown, $R(P,T)$ measurements have also been carried out.

II. EXPERIMENTAL

Stoichiometric amounts of $PdCl_2$ powder and metallic iron foil were heated to 700 °C in an evacuated quartz tube. Pure dry Cl_2 vapor was produced from *in situ* decomposition of $PdCl_2$ and reacted with nearby Fe to produce microcrystals of transparent anhydrous $FeCl_2$. Because of the high deliquescence of the $FeCl_2$, the sample had to be treated and loaded into the diamond-anvil cell [Tel Aviv University miniature opposing-plates diamond anvil cell (DAC) (Ref. 13)] under exceptionally dry conditions using a special glove box. Samples for XRD studies were loaded in a 100 μm diameter by 30–40 μm thickness cavity drilled in rhenium gaskets. Argon was used as a pressurizing medium. The sample for resistivity studies was loaded using a stainless-steel gasket coated with Al_2O_3 into which a sample cavity of ~100 μm diameter was drilled. The quality of the pressurized samples was verified by MS and XRD.

Four-probe direct current (DC) electrical-resistance measurements $R(P,T)$ were carried out using 5–7-μm-thick Pt-foil electrodes. For each pressure the DAC was gradually lowered into a partially filled liquid N_2 Dewar whose gas temperature varied with height to obtain $R_P(T)$ measurements. Sample temperatures were determined from an attached Si-diode thermometer.

HP-XRD studies were performed up to 65 GPa in the angle-dispersive mode at the ID30 beam line of the *European Synchrotron Research Facility*, Grenoble. Two series of measurements were performed at $\lambda=0.4246$ and 0.3644 Å wavelengths, and diffraction images were collected using image plates. The image data were integrated using the FIT2D program[14,15] and the resulting diffraction patterns were analyzed with the GSAS (Refs. 16 and 17) program. The uncertainties in the lattice parameters reported in Table I are solely from the GSAS fitting output. Pressures were measured using the ruby-fluorescence technique.

III. RESULTS

A. Electrical resistance

The pressure variation in R at room temperature is shown in Fig. 2. As can be seen, a drastic decrease occurs between 38 and 45 GPa in which $R(P)$ is reduced by about 4 orders of magnitude. Temperature dependence of the resistance for $P \geq 45$ GPa is shown on the inset. The $R_P(T)$ data at these pressures, e.g., the positive slope of $(\partial R/\partial T)_{P\geq 45\ \mathrm{GPa}}$ is strong evidence for the metallic nature of the HP phase. This result is in concert with the magnetic collapse observed by MS (Ref. 12) thus unequivocally assigning this electronic/magnetic transition to a correlation breakdown and that magnetism collapse is not due to a HS-LS transition, as seen in all Fe-O species studied so far.

B. XRD

As mentioned, at 0.6 GPa $FeCl_2$ undergoes a structural phase transition to a hexagonal h-$FeCl_2$ phase with the CdI_2-type structure, consisting of a sequence of Cl-Fe-Cl, Cl-Fe-C, layers (Fig. 1). This structure can be completely characterized within the hexagonal setting by the two lattice parameters a and c, the iron position at (0,0,0), and the chlorine position at $\pm(1/3,2/3,u)$. Diffraction patterns recorded in the 0–65 GPa pressure range are shown in Fig. 3. The pressure ranges, 0.6–30, 30–58, and 32–65 GPa, characterized by their structural and electronic[12] features, were designated as *low pressure* (LP), *intermediate pressure*, and *high-pressure* (HP) phases. Values of the molar volume $V(P)$,

TABLE I. The refined structural parameters of CdI_2-type phases of $FeCl_2$ at various pressures (Ref. 23)

Pressure (GPa)	a (Å)	c (Å)	u	c/a
		LP phase		
0.62[10]	3.585	5.735	0.239	1.5997
2.6	3.5429(5)	5.502(5)	0.248(2)	1.553(1)
5.6	3.4865(2)	5.361(2)	0.256(2)	1.538(2)
7.6	3.4482(2)	5.284(1)	0.264(1)	1.532(1)
10.1	3.4188(3)	5.221(1)	0.270(2)	1.527(7)
16.5	3.3516(4)	5.062(2)	0.275(2)	1.510(2)
19.4	3.3331(6)	4.974(3)	0.278(1)	1.492(2)
22	3.2999(5)	4.940(3)	0.280(1)	1.497(3)
24.6	3.2893 (5)	4.908(3)	0.279(1)	1.492(1)
28.3	3.2661(4)	4.887(2)	0.279(1)	1.496(2)
		IP phase		
32	3.1417(7)	5.073(4)	0.281(2)	1.615(2)
34.4	3.111(4)	5.087(3)	0.282 (2)	1.635(1)
40.2	3.0924(4)	4.988(7)	0.281(3)	1.613(2)
43.1	3.0846(4)	4.935(12)	0.282(4)	1.600(4)
44	3.0665(3)	4.957(4)	0.276(5)	1.616(7)
48.9	3.0464(7)	4.87(1)	0.280(3)	1.598(4)
53	3.0096(3)	4.87(1)	0.286(2)	1.617(4)
57.1	2.9972(8)	4.78(1)		1.6(1)
		HP phase		
32	3.1906(7)	4.719(8)	0.283(2)	1.479(3)
34.4	3.1571(4)	4.730(4)	0.280(3)	1.498(1)
40.2	3.1374(5)	4.665(2)	0.282(3)	1.487(1)
43.1	3.1379(7)	4.627(2)	0.286(3)	1.474(1)
44	3.1164(5)	4.607(2)	0.280(4)	1.478(9)
48.9	3.1156(5)	4.521(2)	0.282(3)	1.451(3)
53	3.085(1)	4.487(9)	0.282(5)	1.454(4)
57.1	3.0827(2)	4.389(1)	0.283(2)	1.424(1)
61.2	3.0746(2)	4.359(1)	0.284(1)	1.418(6)
64.1	3.0672(2)	4.324(1)	0.284(1)	1.410(5)

$c/a(P)$, $c(P)$, and $a(P)$ are shown in Figs. 6 and 7. Results of the IS(P) which is a measure of the electron density at the Fe site are also shown in Fig. 6.

1. LP phase

Within the 0.6–30 GPa range, the diffraction patterns were satisfactorily fitted with the CdI_2 structure (Fig. 4) resulting in $w_{Rp}<2.7\%$, $Rp<1.9\%$, chi^2 in the range of 0.25–1.3, and $R(F^2)$ in the range of 0.11–0.23. Parameters $V(P)$, $c(P)$, and $a(P)$ decrease continuously with pressure increase, reaching values at 30 GPa of $\Delta V/V_0=-0.30$, $\Delta c/c_0=-0.15$, and $\Delta a/a_0=-0.09$, respectively [see Figs. 6(b) and 7]. The numerical results of the refinement are summarized in Table I. It is noteworthy that, similar to FeI_2,[8] the chlorine coordinate u shows a clear trend to increase with pressure. The c/a value decreases monotonically with pressure from 1.6 to 1.5

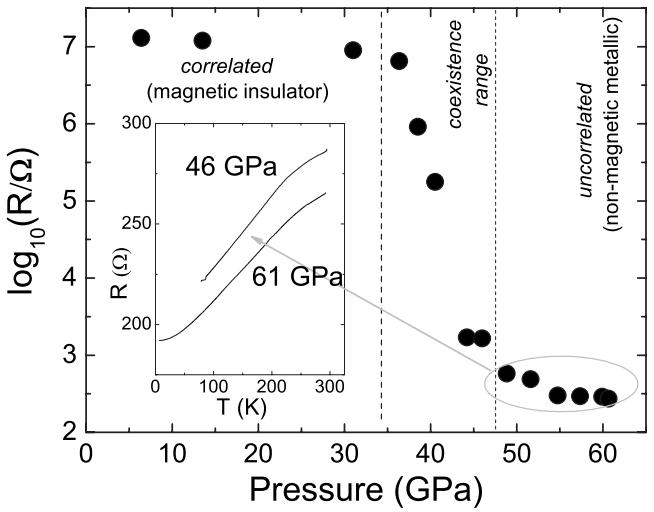

FIG. 2. Pressure dependence of the resistance at 300 K. Note the sharp decrease in R, by about 4 orders of magnitude, starting in the 35–47 GPa intermediate range. For $P>47$ GPa the metallization process is complete. The metallic behavior is clearly evident at these pressures as shown in the inset.

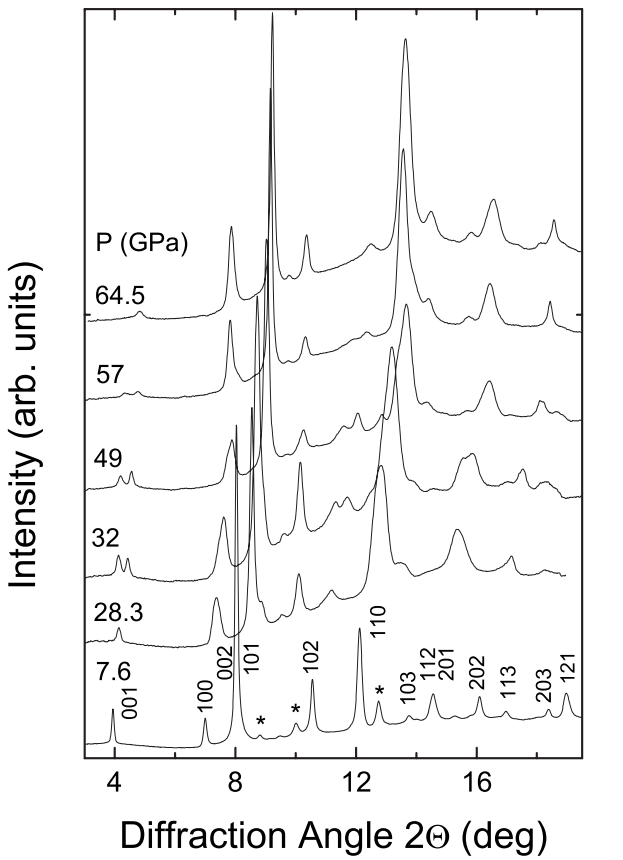

FIG. 3. XRD powder-diffraction patterns of $FeCl_2$ at RT at various pressures. Note the distinctive splitting of the diffraction peaks at 32 GPa, especially the (001) and (102) lines. Above 60 GPa this splitting disappears. The peaks marked with an asterisk correspond to the Re gasket.

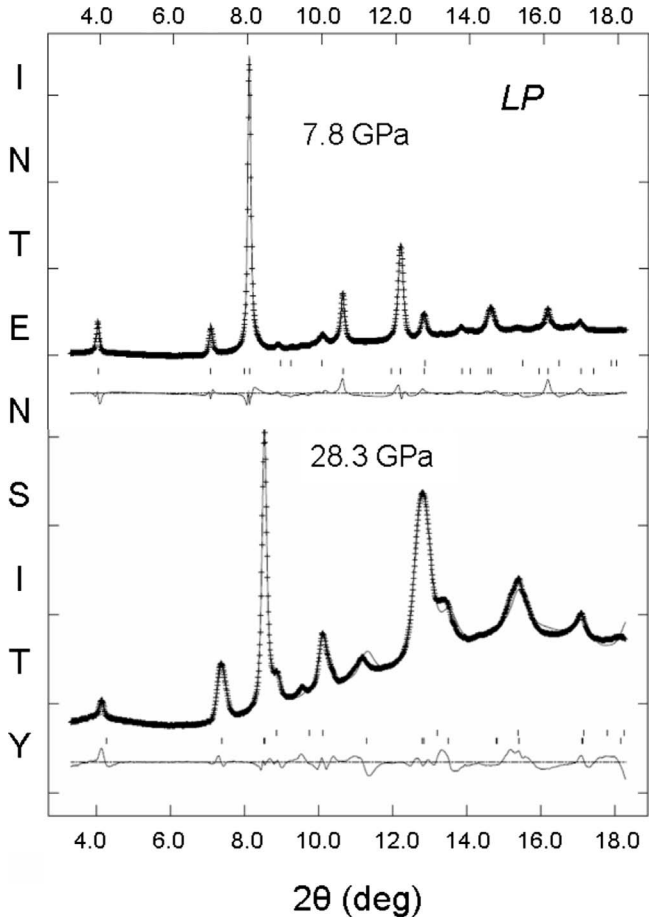

FIG. 4. Typical examples of analyzed integrated patterns collected for the LP phase: 7.8 and 28.3 GPa (LP–lower tick set and Re gasket–upper tick set) using the CdI_2-type structure. The GSAS program package was used.

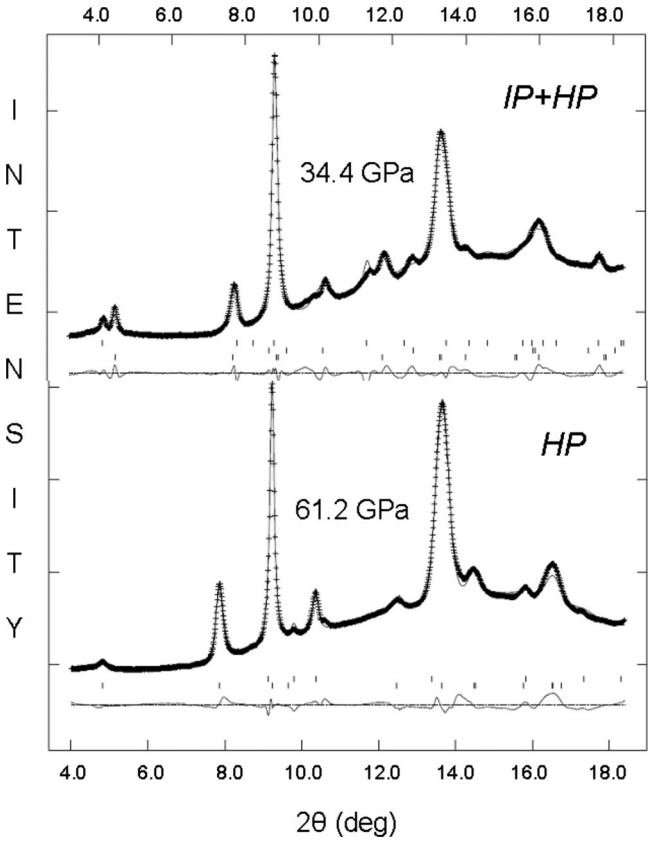

FIG. 5. Typical examples of analyzed integrated patterns collected at: 34.4 (HP–lower ticks, Re gasket–middle ticks, and IP–upper ticks) and 61.2 GPa (HP–lower ticks and Re gasket–upper ticks), assuming a CdI_2-type structure.

which we attribute to the soft anisotropic compression along the c axis.

2. IP phase

At $P \geq 32$ GPa a significant asymmetric broadening of the (100), (101), (110), (201), and splitting of the (001), (102) diffraction peaks are observed (Fig. 3). At this pressure a good quality fit could be obtained assuming coexistence of two *isosymmetrical* phases albeit with different atomic parameters (see Fig. 5). The one characterized by larger c and reduced a parameters was designated as intermediate-pressure phase (abundance ~85% at 32 GPa). The c/a value exhibits a discontinuous 8% increase at the LP→IP transition edge and attains a value of 1.63 similar to that of the ambient pressure modification of $FeCl_2$.[10] Within the statistical error the $V(P)$ shows no discontinuity at the LP→IP interface.

The combined $V(P)$ data for both LP and IP (Fig. 6) could well be fitted with a single Birch-Murnaghan equation[18]

$$P = 1.5K_0[(V_0/V)^{7/3} - (V_0/V)^{5/3}] \times [1 - 0.75(4 - K_0')\{(V_0/V)^{2/3} - 1\}], \quad (1)$$

with the following parameters: K_0=35.3(1.8) GPa, K_0'=4 (fixed), and V_0=64.7(0.8) Å^3 where K_0, K_0', and V_0 are the bulk modulus, its pressure derivative, and the unit-cell volume at ambient conditions, respectively.

3. HP phase

Another phase which appears above 32 GPa was designated as the HP modification. This new phase coexists with the IP phase (34 GPa in Fig. 5) and its relative abundance, based on the GSAS fitting, increases sluggishly with rising pressure, reaching 100% at ~60 GPa. It was possible to fit the HP diffraction data within the CdI_2 structure. The result of a refinement obtained in the 32–65 GPa range is summarized in terms of $V(P)$, $c(P)$, and $a(P)$ [Figs. 6(b), 7(b), and 7(c)]. One can see that the transition to the HP phase is accompanied by a discontinuous reduction in volume (~3.5%) and c (~7%), as well as by a slight increase in a and consequently the c/a ratio drops by ~8% [Fig. 7(a)]. $V_{HP}(P)$ could well be fitted with the Birch-Murnaghan equation (1) yielding: K_0=36.2(5.1) GPa, K_0'=4 (fixed), and V_0 =62.2(2.6) Å^3.

4. Atomic distances

The P dependencies of the interatomic distances are shown in Fig. 8. One can see that in the LP and IP phases the pressure primarily reduces the empty space between the Cl-

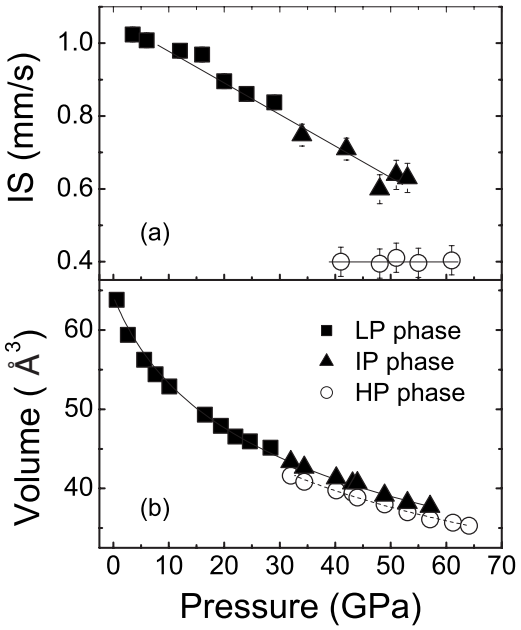

FIG. 6. (a) Pressure dependence of the IS (Ref. 11) of ^{57}Fe showing a continuous decrease with pressure with no discontinuity in slope while passing through the LP-IP phase. An abrupt decrease is observed at the crossover of the correlated with uncorrelated regimes. $\rho_s(0)$, the *s*-electron density at the nucleus (proportional to IS in ^{57}Fe) increases with P and a discontinuous increase at the HP phase crossover. (b) Pressure dependence of unit-cell volume. The solid and dotted lines are the theoretical fit for the combined LP-IP and HP phases, respectively, using the Birch-Murnaghan formula for the equation of state. The transition to the HP phase is accompanied by a volume reduction of ~3.5%.

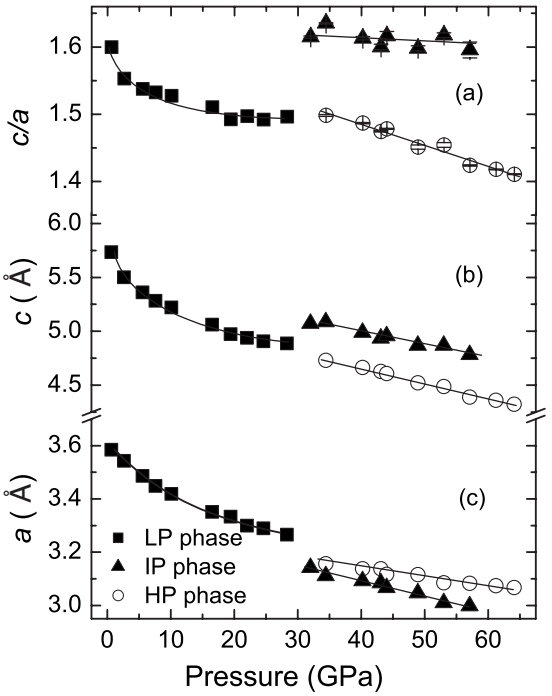

FIG. 7. (a) Pressure dependency of the $FeCl_2$ crystal anisotropy reflected by the c/a ratio. The highest discontinuous increase in c/a occurs at the onset of the IP phase. [(b) and (c)] The $c(P)$ and $a(P)$ plots show a discontinuous increase in the c axis by ~0.2 and a decrease in the a axis by 0.13 Å. In the HP phase the sign of the parameter change is reversed.

Fe-Cl layers, namely, the Cl-Cl interlayer distances, while the Fe-Cl and Cl-Cl intralayer distances also decrease with pressure but not as severely as the c parameter. Following the LP-IP transition we observe no discontinuity in the Cl-Cl interlayer distances nor in the Fe-Cl bond length, whereas the Cl-Cl intralayer distances increase appreciably (~2.7%), concurrently with decrease in the Fe-Fe distances (~3.5%). This signals a significant lattice distortion in the c direction. Following the IP-HP transition, changes in atomic distances occur both within and between the layers: (i) at the intralayers a discontinuous decrease in the Fe-Cl bond lengths (~1.4%) is observed in concert with the shortening of the Cl-Cl distances (~4.1%), the Fe-Fe distances increase by ~1.3%, and (ii) the interlayer Cl-Cl distances decrease by 3%.

IV. DISCUSSION AND CONCLUSIONS

A. Mössbauer studies of the electronic phase transitions

1. Electronic LP phase

Within the range of 0–30 GPa, the hyperfine field is composed of two main terms:[12,19] the *Fermi-contact* term, proportional to the difference of the spin-up and spin-down densities at the nucleus, and the *orbital* terms

$$H_{\mathrm{hf}} = -\,\mathrm{const}\ \mu_B[\rho_s^{\uparrow}(0) - \rho_s^{\downarrow}(0)] + 2\mu_B\langle r^{-3}\rangle\langle I_z\rangle, \qquad (2)$$

where I_z is the z component of the *orbital* angular momentum. At ambient pressure $H_{\mathrm{hf}} \sim 2.5$ T reaching a maximum of 5 T at 18 GPa. At ~32 GPa it jumps to 35 T, typical of a Fe^{2+} hyperfine field arising from a pure Fermi-contact term. At this range the IS decreases [$\rho_s(0)$ increases] gradually (Fig. 6). This jump in H_{hf} results from the quenching of the orbital term, coinciding with the onset of the IP phase as detected by XRD.

2. IP phase

The electronic IP phase is characterized by the realignment of the magnetic moments from 0° to ±55° with respect to the c axis.[12] No discontinuity in IS is observed at the LP-IP interface, and IS(P) maintains its continuous decrease. Unlike FeI_2, where T_N increases abruptly from 150 to 260 K upon quenching of the orbital term,[6] no discontinuous increase is observed in $FeCl_2$.[12]

3. HP phase

With ^{57}Fe Mössbauer spectroscopy the HP phase is first detected above 38 GPa. This electronic phase is characterized by discontinuous decreases in IS(P) [increase in $\rho_s(0)$] and quadruple splitting (QS) and a total collapse of magnetization. The IP coexists with the HP phase until ~60 GPa with IS and QS holding practically constant.

B. Structural response to the LP-IP-electronic phase transition

Structural response to the LP→IP electronic phase transition is quite unique. No symmetry change is detected at the

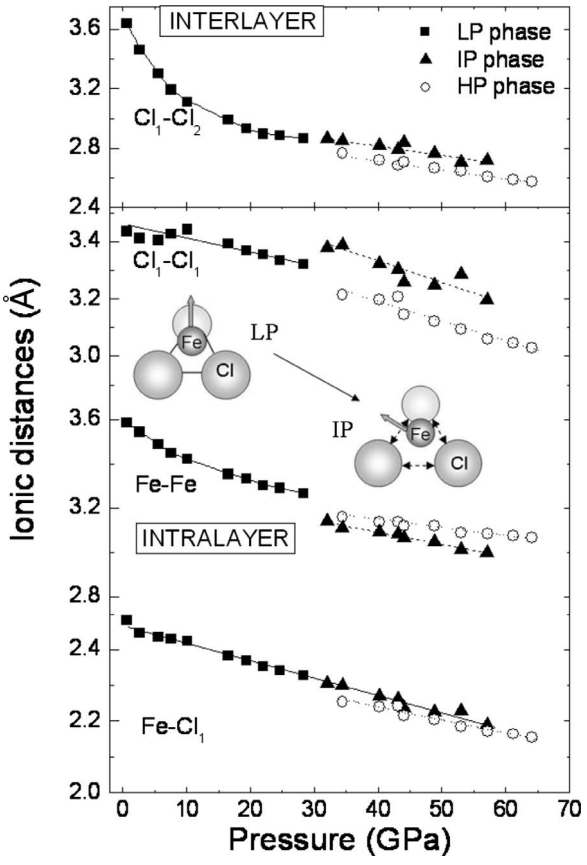

FIG. 8. Ionic distance evolution with pressure increase in intralayer Cl_1-Cl_1, Fe-Fe, and Fe-Cl, and interlayer Cl_1-Cl_2 distances. One can see that in the LP phase up to ~20 GPa the pressure primarily reduces the interlayer Cl_1-Cl_2 distances, leaving the layer itself rather rigid. At higher pressures whereas the Fe-Cl bond length is barely affected by the LP-IP transition this is not the case of the intralayer Cl_1-Cl_1. The "spreading" of the Cl-Cl distances corroborates with the orbital quenching and the consequent tilting of the Fe^{2+} moment by 55° (see text) shown in the two sketches of the Fe-Cl_3 tripyramid. At the IP→HP transition a discontinuous decrease in the Fe-Cl bond lengths is observed in concert with the shortening of the intralayer Cl-Cl distances.

LP-IP phases interface and no discontinuity in $V(P)$ nor in $\rho_s(0)(P)$ are observed [Figs. 6(a) and 6(b)]. However, one observes a discontinuous shrinkage of the a axis with an expansion of the c axis leading to a large increase in the c/a value, namely, a corresponding increase in anisotropy [see Fig. 6(a)].

On the atomic scale, one observes an intralayer Cl-Cl spacing increase at the LP-IP interface. To compensate for the unaffected Fe-Cl bond length, the Fe-Fe distance will have to contract. Similar intralayer atomic reorganization was observed recently in FeI_2 concurring with the offset of the *spin-orbit term*. The fact that in both systems the crystallographic LP→IP transition and the quenching of the orbital term take place at the same pressure range with no volume nor IS (Ref. 20) changes gives rather strong evidence that the observed lattice distortion in the c direction, at the IP phase, is indeed *attributed to the quenching of the orbital term*. Recently Kunes *et al.*,[21] based on electronic-structure calculations for FeI_2, infer that the experimentally observed vanishing of the orbital moment originates from a pressure-induced change in the symmetry of the occupied minority-spin d orbital, namely, change from twofold-degenerate e_g' orbital to a_g occupation. The latter orbital is characterized by very strong anisotropy of the charge and spin distributions with the angular part stretched along the c axis. This is in good agreement with the present observed lattice distortion in the c direction. We note that all these changes do not affect the interlayer bond distances.

It is noteworthy that the consequence of the quenching of the orbital term upon T_N is not straightforward: (i) a significant increase in the ferrous-ion moment leads to an enhanced superexchange interaction and a corresponding increased T_N value, (ii) but the abrupt increase in the c parameter tends to reduce the antiferromagnetic coupling along this direction and diminish T_N. The competition of these two factors will determine any change in T_N at the LP-IP transition. In FeI_2, where lattice distortion is relatively weak ($\Delta(c/a) \approx 5\%$),[8] as compared to $FeCl_2$ ($\Delta(c/a) \approx 8\%$), the first factor dominates and T_N increases significantly.

C. Structural response to the IP-HP electronic phase transition

The HP phase is created following a structural first-order transition. Although no symmetry change occurs, there is a volume contraction by ~3.5% on par with a discontinuous decrease in the IS [Fig. 6(a)]. The pressure extent of the HP-IP coexistence is remarkable. Diffraction lines of the HP phase are detected at pressure as low as 32 GPa, practically coinciding with the onset of IP whereas with MS the HP phase appears above 38 GPa.[12,19] The HP abundance grows at the expense of the IP phase and above 62 GPa only the metallic-nonmagnetic HP phase remains. The large pressure range of coexistence suggests that the energy gap between the two phases is rather small; requiring a reduction $\Delta V/V$ in ~0.14 to fully complete IP→HP conversion.

During this sluggish pressure-induced process an important physical occurrence takes place. Within the HP phase a breakdown of the *charge-transfer* correlation takes place resulting in a considerable decrease in the Fe-Cl bond length and the Cl-Cl interlayer distances, concurrent with the onset of free electrons. The equal values of K_0^{IP} and K_0^{HP} implies that the reduction in Fe-Cl bond length and the onset of metallization barely affect the phonon density of state.

Considering the parameters obtained from the fitting of the HP equation of state (EOS): $K_0 = 36.2(5.1)$ GPa and $V_0 = 62.2(2.6)$ Å^3, one concludes that bulk modulus K_0 of the IP and HP phases are equal, within the statistical error; however there is a significant reduction of ~3.5% in molar volume. It is obvious that the factor responsible for the discontinuous decrease in V_0^{HP} is the reduction in ~1.5% in Fe-Cl bond length and the decrease in ~3% in the Cl-Cl interlayers distances upon correlation breakdown. In addition to the above mentioned alterations of bond distances, a significant change in the lattice distortion takes place at the IP-HP transition. The unit-cell contracts in the c direction and this distortion change has almost the same absolute value but an

opposite sign as compared to the LP-IP case [see Fig. 7(b)]. This signals a possible reversal to the LP symmetry of the occupied minority-spin *d* orbital, namely, return to e_g' occupation, which is characterized by a less anisotropic charge and spin distribution.

The substantial reduction in Fe-Ha (Ha=Cl,I) distances both in the chloride and iodide suggest that the halide *p* bands play an important role in the insulator-metal transition. This implies that the mechanism of the correlation breakdown is the CT gap closure, e.g., the pressure-induced overlap of the Ha 3*p* band with the Fe 3*d* upper band.

The CdI_2 structure shows a high resiliency to the PI electronic transitions to 70 GPa, starting with the response to the *d*-orbital term quenching, manifesting itself by the significant change in the lattice anisotropy, and ending with an insulator-metal transition and a discontinuous reduction in the molar volume. A similar resiliency to electronic pressure-induced transitions to $P=170$ GPa has been reported for the case of $R\mathrm{Fe}^{3+}\mathrm{O}_3$ ($R\equiv$rare earth) perovskites.[22]

Finally, it is worth emphasizing two structural phenomena occurring at the *intermediate phase*, common to the FeHa_2 species, and associated with the electronic transitions: (i) a substantial change in the lattice distortion coinciding with the quenching of the orbital moment term and (ii) an intermediate structural precursor signaling the electronic-correlation breakdown.

ACKNOWLEDGMENTS

This research was supported in part by the Israeli Science Foundation under Grant No. #36/05. Some of experiments were performed at the Bayerisches Geoinstitut under the EU "Research Infrastructures: Transnational Access" Programme under Contract No. 505320 [(RITA)–High Pressure]. We thank G. Yu. Machavariani for assisting with the resistivity measurements.

[1] N. F. Mott, *Metal-Insulator Transitions*. (Taylor & Francis, London, 1990) and references therein.

[2] M. P. Pasternak, R. D. Taylor, R. Jeanloz, X. Li, J. H. Nguyen, and C. A. McCammon, Phys. Rev. Lett. **79**, 5046 (1997).

[3] Resistance measurements in FeO to 150 GPa showed no evidence of an insulator-metal transition asserting that the magnetism collapse followed a HS-LS transition. See S. T. Weir, J. Akella, Y. K. Vohra, S. A. Catlidge, K. Gandehari, and C. Ruddle, *Science and Technology of High Pressure*, Proceedings of the International Conference on High Pressure Science and Technology, Honolulu, Hawaii, 25–30 July, 1999, edited by M. H. Manghnani, W. J. Nellis, and M. F. Nicol (Universities Press, Hyderabad, India, 2000), Vol. 1, p 82.

[4] M. S. Speziale, A. Milner, V. E. Lee, S. M. Clark, M. P. Pasternak, and R. Jeanloz, Proc. Natl. Acad. Sci. U.S.A. **102**, 17918 (2005).

[5] S. Takele and G. R. Hearne, Phys. Rev. B **60**, 4401 (1999).

[6] M. P. Pasternak, W. M. Xu, G. Kh. Rozenberg, R. D. Taylor, G. R. Hearne, and E. Sterer, Phys. Rev. B **65**, 035106 (2001).

[7] M. P. Pasternak, R. D. Taylor, A. Chen, C. Meade, L. M. Falicov, A. Giesekus, R. Jeanloz, and P. Y. Yu, Phys. Rev. Lett. **65**, 790 (1990).

[8] G. Kh. Rozenberg, M. P. Pasternak, W. M. Xu, L. S. Dubrovinsky, J. M. Osorio Guillén, R. Ahuja, B. Johansson, and T. Le Bihan, Phys. Rev. B **68**, 064105 (2003).

[9] J. C. Slater, *Quantum Theory of Molecules and Solids* (McGraw-Hill, New York, 1963), Vol. 1.

[10] C. Vettier and W. B. Yelon, J. Phys. Chem. Solids **36**, 401 (1975).

[11] D. J. Simkin, Phys. Rev. **177**, 1008 (1969).

[12] W. M. Xu and M. P. Pasternak, Hyperfine Interact. **144–145**, 175 (2002).

[13] E. Sterer, M. P. Pasternak, and R. D. Taylor, Rev. Sci. Instrum. **61**, 1117 (1990).

[14] A. P. Hammersley, ESRF Internal Report No. ESRF97HA02T, 1997 (unpublished).

[15] A. P. Hammersley, S. O. Svensson, M. Hanfland, A. N. Fitch, and D. Hausermann, High Press. Res. **14**, 235 (1996).

[16] A. C. Larson and R. B. Von Dreele, Los Alamos National Laboratory Report No. LAUR 86–748, 1994 (unpublished).

[17] B. H. Toby, J. Appl. Crystallogr. **34**, 210 (2001).

[18] O. L. Anderson, *Equations of State of Solids for Geophysics and Ceramic Science* (Oxford University Press, Oxford, 1995).

[19] We note that there are slight differences in determining the pressure limits of LP, IP, and HP between the current XRD and the previous MS studies. One of the reasons is the higher Signal/Background sensitivity of the synchrotron XRD (SXRD) method allowing detection of new components at a level where its relative abundance is too small for effective MS. Another reason is the different geometry of the signal collection: for SXRD the signal comes from a small central part of the sample, whereas in MS studies the signal is collected from almost the whole sample diameter and may reflect an appreciable pressure gradient.

[20] A drop in IS in ^{57}Fe, which is *negatively* proportional to the increase in the *s*-electron density at the Fe nucleus, usually follows a volume reduction (see Ref. 2).

[21] J. Kunes, H. Rosner, D. Kasinathan, C. O. Rodriguez, and W. E. Pickett, Phys. Rev. B **68**, 115101 (2003).

[22] W. M. Xu, O. Naaman, G. Kh. Rozenberg, M. P. Pasternak, and R. D. Taylor, Phys. Rev. B **64**, 094411 (2001); G. Kh. Rozenberg, M. P. Pasternak, W. M. Xu, L. S. Dubrovinsky, S. Carlson, and R. D. Taylor, Europhys. Lett. **71**, 228 (2005).

[23] The error bars of the lattice parameters were obtained from the GSAS program. We are aware that apart of the statistical errors obtained from the program there are additional sources of systematic errors that are not taken into account. Errors arising from possible strains, texture, and pressure distribution are not available, and are not included.